Remarks on a multiscale approach to grain growth in polycrystals

Katayun Barmak, David Kinderlehrer, Irine Livshits and Shlomo Ta'asan

Abstract. Nearly all technologically useful materials are polycrystalline. Their ability to meet system level specifications of performance and reliability is influenced by the types of grain boundaries present and their connectivity. To engineer the grain boundary network to achieve these objectives, we seek predictive models of growth at various mesoscale levels. Here we discuss a master equation description of normal grain growth derived from large scale simulations and compare the results with recent experiments.

Introduction

A central problem in materials science is the understanding and control of microstructure, the ensemble of grains that comprise polycrystalline materials. Macroscopic properties of these materials are affected by grain size, texture and other mesoscale properties. The orientations and arrangements of the grains and their network of boundaries are implicated in many properties across wide scales, for example, functional properties, like conductivity in microprocessors, and lifetime properties, like fracture toughness in structures. Modeling and simulation of the grain evolution at the mesoscale plays an increasingly important role in resolving this central problem. With the implementation of automated data acquisition, based on orientation imaging microscopy, in the Mesoscale Interface Mapping Project, a strategy has emerged for determining interfacial energy and mobility in polycrystals, [1]. Our present task is to investigate microstructural evolution.

Here we examine the issues related to simulations of grain boundary network evolution subject to the conventions of normal grain growth and compare these

This work was supported in part by the MRSEC program of the National Science Foundation under Award Number DMR-0079996 and by DMS 0305794
To appear in Prog. Nonlinear Diff. Eqns and Appl. vol 68, 1-11, 2006.

with new experimental work on aluminum thin films. Normal grain growth consists of the Mullins Equations of curvature driven growth [16, 10] in a two-dimensional setting with appropriate boundary conditions at triple junctions, where boundaries meet. This paradigm system is the most studied in theory and corresponds in experiment to a columnar grain structure, which is what we shall actually see in the experiment. Are there general laws of evolution for ensembles of grains? Such questions have been studied for many generations and now become accessible by means of a very large scale reliable and accurate approach to simulation.

To engage this issue we are led to another. The simulated coarsening process is a large metastable system with a precise formulation, for example, consisting of some 50,000 nonlinear partial differential equations. This must be replaced at a larger scale by some distribution functions, or stochasticized, in order to be interpreted. Which distribution functions to choose may be a matter of history, art, or intuition, but there remains the necessity of deriving their stability and robustness. The problem, after all, is all mathematics. The issue is yet more compelling since we are ultimately asked to compare the simulation with experimental results. We are not able to directly pass from the mesoscopic scale of the simulation to the more macroscopic scale, but we shall seek to derive some theory for the distribution functions which is simulation based. This vast multiscale arena has many challenges.

1. Recapitulation of grain growth

We review very briefly the Mullins Equation for the evolution of a two dimensional grain boundary system. Our concern here is limited to systems with constant energy and mobility. Consider a curve family, or an evolving curve,

$$\Gamma : x = \xi(s,t), \quad 0 \leqq s \leqq L, \ t > 0, \tag{1.1}$$

with

$$b = \frac{d\xi}{ds} \ (tangent) \ \ and \ \ n = Rb \ (normal).$$

Let γ denote the energy density and μ the mobility of Γ. The equation of motion is then

$$v_n = \mu\gamma\kappa \ \ on \ \Gamma, \quad \kappa = curvature \tag{1.2}$$

We assume that only triple junctions are stable and impose the Herring condition, [10], where three curves meet. This condition reduces to: if $\Gamma^{(1)}, \Gamma^{(2)}, \Gamma^{(3)}$ meet at p, then they meet at angles of $2\pi/3$. It is the natural boundary condition in equilibrium for the functional

$$F = \sum_{i=1..3} \int_{\Gamma_i} \gamma ds$$

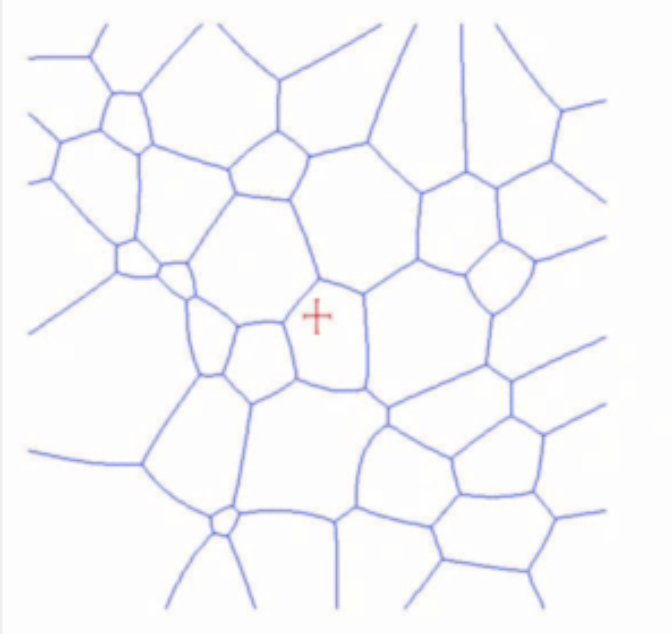

FIGURE 1. A snapshot of a network of grain boundaries from the simulation

under the asumption that the three curves meet at the triple junction p. Consider a network of grains bounded by $\{\Gamma_i\}$ subject to some conditions at the border of the region they occupy, like fixed end points or periodicity, cf. Figure 1. The total energy of this system

$$E(t) = \sum_{\{\Gamma_i\}} \int_{\Gamma_i} \gamma ds$$

during evolution in the absence of topological events satisfies

$$\frac{d}{dt} E(t) \leqq 0,$$

and thus the system is dissipative. Our simulation is designed to preserve this feature at the discrete level and to enforce it during topological events, [14].

The well posedness of [16] with the Herring condition was discovered by [5] and long time existence established in [11]. Details of the simulation method may be found in [13], [14].

2. Master equation approach to evolution

The idea of the master equation approach is to replace the original mesoscale system of many equations with a simpler set of equations that still provides desired information. In this implementation, the connectivity of the grain bounday network is abandoned in favor of side class distributions motivated by the Mullins-von Neumann $n-6$ rule. The strategy is to discover such a system of equations by interrogating the simulation, a strategy made possible because we have at hand a reliable large scale simulation. As suggested, here we are primarily interested in the stationary relative area histogram.

Suppose a grain with n sides or facets evolves subject to [16] and the Herring Condition. Then, according to the Mullins-von Neumann Rule, 16 and also von Neumann in [17], its area $A(t)$ satisfies

$$\frac{d}{dt}A(t) = \alpha(n-6), \quad t>0, \quad \alpha = \frac{\pi}{3}\mu\gamma. \tag{2.1}$$

A grain is subject to events which may increase or decrease its number of sides, usually called topological events or critical events, so through its history, we may think of a given grain with area x as satisfying an equation like

$$\frac{d}{dt}x(t) = \alpha(n(t)-6), \quad t>0, \tag{2.2}$$

where $n(t)$ may increase or decrease by 1 at a time at various times and if $x(t)=0$, the grain is deleted from the system. Thus $x(t)$ is like the sample path of a stochastic process. Deducing a master equation for the ensemble of grains based on this notion does not seem possible, but the perception that there should be such a master equation is what motivates our thinking.

Let

: $f_n(x,t)$ be the density of n-sided grains with area x at time t,
: $g_n(t) = \int_0^\infty f_n(x,t)dx$ density of grains with n-sides surviving at time t,
: $g(t) = \sum g_n(t)$ density of (surviving) grains at time t.

In a time interval during which n-sided grains experience no topological changes, $(T, T+\tau)$, the density f_n changes only through transport so

$$\frac{\partial f_n}{\partial t} + \alpha(n-6)\frac{\partial f_n}{\partial x} = 0, \quad x>0,\ T<t<T+\tau$$

which leads us to seek a system of equations of the form

$$\begin{aligned} \frac{\partial f_n}{\partial t} + \alpha(n-6)\frac{\partial f_n}{\partial x} &= A_{nn-1}f_{n-1} + A_{nn}f_n + A_{nn+1}f_{n+1}, \\ & x>0,\ t>0, n = n_{min}, ..., n_{max} \\ f_n(0,t) &= 0, \quad t>0, n = 6, ..., n_{max} \end{aligned} \tag{2.3}$$

satisfying the conservation conditions

$$\sum_{n_{min} \leqq i \leqq n_{max}} A_{ij} = 0, \quad and \quad A_{ii-1} \geqq 0, \; A_{ii} \leqq 0, \; A_{ii+1} \geqq 0 \tag{2.4}$$

We take $n_{min} = 3$ and typically in simulation $M \equiv n_{max} = 11$ or 12. The equations (2.3) have the appearance of a birth/death process with transport; for sufficiently small $\tau > 0$,

$$\mathbf{1} + \tau A, \quad A = (A_{ij})$$

is a probability matrix.

On this basis, we may make several quick observations. Assume that

$$\begin{aligned} A_{nn-1} &> 0, \quad 3 < n \leqq M \\ A_{nn} &< 0, \quad 3 \leqq n \leqq M \\ A_{nn+1} &> 0, \quad 3 \leqq n < M \end{aligned}$$

and that $f_n(x, 0) \geqq 0$. Then $f_n(x, t) \geqq 0$, since at the first time t where $f_n(x, t) = 0$ for some x, f_n has a minimum, so $\partial f_n / \partial t \geqq 0$ and f_n is increasing. Now suppose that n-sided grains are extinguished at some time t_0, namely,

$$f_n(x, t_0) = 0, \quad x > 0, \quad some \; fixed \; t_0$$

Then

$$\frac{\partial f_n}{\partial t} = \frac{\partial f_n}{\partial x} = 0$$

and

$$A_{nn-1} f_{n-1} + A_{nn+1} f_{n+1} = 0$$

so $f_{n-1} = f_{n+1} = 0$, and so forth, whence the solution is extinguished for time $t \geqq t_0$. These arguments may be refined and, essentially, have to do with the ergodicity of the Markov Chain with matrix $\mathbf{1} + \tau A$. We shall not actually be entitled to impose the conditions above on A, but we believe the conclusions to hold nonetheless.

There are two special constraints on (2.3) and (2.4). From the Euler formula (♯ polygons - ♯ edges + ♯ vertices = 1), the average number of sides per grain in the network is 6 since curves can meet only at triple junctions, except for a small number on the outside border, cf. Smith [17]. Assuming this for the initial conditions, we then need that

$$\frac{d}{dt} \sum_n (n - 6) \int_0^\infty f_n dx = 0$$

Now,

$$\begin{aligned}\frac{d}{dt}\sum_n (n-6)\int_0^\infty f_n dx &= \sum_n (n-6)^2 \int_0^\infty \frac{\partial f_n}{\partial t} dx \\ &= -\alpha \sum_n (n-6)^2 \int_0^\infty \frac{\partial f_n}{\partial x} dx + \sum_{nj} (n-6)\int_0^\infty A_{nj} f_j dx \\ &= \alpha \sum_3^5 (n-6)^2 f_n(0,t) + \sum_{n,j} (n-6)\int_0^\infty A_{nj} f_j dx\end{aligned}$$

Hence, since only grains with 3,4, or 5 sides can vanish,

$$\alpha \sum_3^5 (n-6)^2 f_n(0,t) = -\sum_{n,j} (n-6)\int_0^\infty A_{nj} f_j dx \tag{2.5}$$

Secondly, the total area of the configuration remains constant, so

$$\sum_n \int_0^\infty f_n x dx = const. \tag{2.6}$$

(2.6) is implied by (2.5). It is also easy to check that

$$\frac{d}{dt} g(t) = \alpha \sum_{\mu=3..5} (\mu - 6) f_\mu(0,t) \leqq 0. \tag{2.7}$$

representing that grains are being deleted from the system. To date, it is the only dissipation we have found in the system. The reciprocal of the proportion of the surviving grains is a measure of the average grain area at time t. We shall use the expression

$$< area(t) >= \frac{g(0)}{g(t)} \tag{2.8}$$

Let us discuss briefly how the matrix A arises from the simulation. There are two possible contributions to non-zero A_{nj}, from grain deletion and from facet switching. Grain disappearance is not a random event, since grains with less than 6 sides tend to vanish, however the grains affected by the vanishing of a given grain may be regarded as having been randomly selected from the ensemble. We limit discussion to grain deletion events in the limited space provided us here.

From (2.1), in a short time τ, a 3,4, or 5 sided grain may disappear. When a 3 sided grain disappears, each of its three neighboring grains loses a side, and, in general, if a μ sided grain disappears, $6-\mu$ sides are lost. Hence the rate of boundaries lost is

$$\psi(t) = \lim_{\tau\to 0}\sum_{3}^{5}\frac{\mu-6}{\tau}\int_0^{\alpha(6-\mu)\tau} f_\mu(x,t)dx \tag{2.9}$$

$$= \alpha\sum_{3}^{5}(\mu-6)^2 f_\mu(0,t) \tag{2.10}$$

consistent with (2.5). This factor is apportioned among the various n in a way determined by interrogation of the simulation. We find that

$$\begin{aligned} A_{nn+1} &= \frac{\psi(t)}{g_{n+1}(t)}a_{n+1} + A^{facet}_{nn+1},\\ A_{nn} &= -\frac{\psi(t)}{g_n(t)}a_n + A^{facet}_{nn},\\ A_{nn-1} &= A^{facet}_{nn-1}, \end{aligned} \tag{2.11}$$

where $a_j \geqq 0$ are *constants* with $a_3 + ... + a_M = 1$. A^{facet}_{nj} refers to the contribution to A_{nj} from facet interchange and it also depends on t alone and this dependence is through g_j and g. In the product

$$A_{nj}f_j(x,t) = \pm\psi_j(t)a_j\ \frac{f_j(x,t)}{g_j(t)} + \ ...$$

the fraction is the probablilty density that a grain of j sides has area x and a_j is the conditional probability that a grain loses a side given that it has j sides. As observed, ψ is a measure of the rate, or number of edges, lost through grain disappearance at time t. Facet interchange can change the side class of a grain but not cause its disappearance. The grains affected by switching are selected randomly from the ensemble. If we compromise and replace the terms g_j and g which occur in denominators by $\epsilon + g_j$ and $\epsilon + g$, then the conclusions based on the ergodicity of the Markov Chain are available to us.

We know little about this system of equations. A first objective is to show that the average grain area (2.8) grows linearly in time. Actually, to our knowledge, none of the grain growth models based on the $n-6$ rule have been shown to have this property. There should, in addition be some form of self-similar solution. This means that the relative area density

$$\rho(x,t) = \frac{1}{g(t)}\sum_{n=3...M} f_n(x,t) \tag{2.12}$$

should have a self-similar form for large t. For a range of parameter values, including those derived from the large scale simulation, this seems reasonable. However this self-similar form may depend on the initial data. Perhaps there is a manifold of self-similar solutions.

We present a few results of simulations. Figure 2 shows $\rho(x,0)$ determined from the initial configuration of the large scale simulation and Figure 3 is a typical comparison of $\rho(x,t)$ computed from the master equations with the histogram gathered from the simulation. The master equation description gives quite good agreement with the large scale simulation. The values near $x = 0$ are nearly coincident and they are in close agreement for $0.4 \leqq x \leqq 1$. This decay as $x \to 1$ is of the form $exp(-\lambda x)$.

The evolution of the relative area histogram may be discussed from a long time standpoint by analyzing data collected at 20 to 25 time steps during the simulation, [12]. This results in a Fokker-Planck equation and thus suggests some diffusion behavior in the system, confirmed by computing that the decay of the sequence of histograms to their stationary state is linearly exponential. Although this may be a consequence of the long time interval separating the histograms, which may allow some details of the statistics to equilibrate, transport systems - if not single transport equations - can exhibit diffusive behavior, [15].

The large scale simulations are insensitive to grain boundary energy, even when it depends on both normal angle and lattice misorientation, and agree well with Monte Carlo type simulations. As we discuss in the next section, they do not compare very well with our recent experiments on Al thin films, which is a columnar structure.

Other derivations of master equation type systems starting from the $n - 6$ rule have been given in the past, eg. by Fradkov, 7, and Flyvbjerg, [6]. They are reviewed in [18].

3. Comparison with experiments

Grain growth was examined in 25 and 100 nm thick films of aluminum deposited onto oxidized silicon wafers. Film texture for the 100 nm thick films was characterized through pole figures and found to be strongly $< 111 >$ fiber-textured, with little strengthening of this texture upon annealing. The grain structure of the films was characterized by transmission electron microscopy. Additional experimental details are given in [2], [3], cf. also [4].

Table 1 gives the mean grain size and its standard deviation as a function of annealing time for the 100 nm thick Al film. It is clear that grain growth stagnates after one hour, when the grains have nearly doubled in diameter from 68 nm to 134 nm. The subsequent evolution is not exactly self-similar, although the various distributions are not greatly different. The main feature is that the relative area histogram is more shifted toward the left and there is an increased fraction of small grains. This indicates that small grains persist in the structure longer than expected. At the same time, the tails of the distributions show a small but significant number of grains 5 to 18 times larger than the mean. By contrast, very few grains are generally found with areas more than 5 times the mean in simulation.

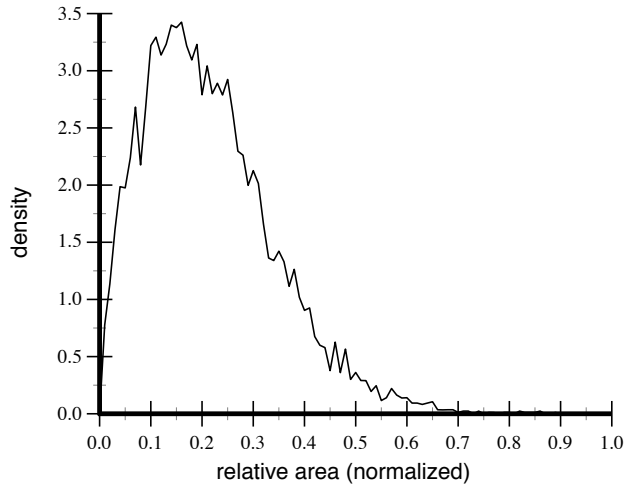

FIGURE 2. Initial relative area histogram gathered from the large scale simulation

Aluminum thin films			
Annealing time (h)	Average radius (nm)	Standard deviation	Number of measured grains
0	68	29	1497
0.5	87	42	1304
1	134	73	1100
2	139	68	1353
4	146	75	1455
10	137	45	2022

TABLE 1. Data for 100 nm thick Al grains annealed at 400^oC.

It is useful to address the issue of stagnation in the thin film. Pinning of grain boundaries by either grooves formed at the film surface or by solute drag has been proposed as a mechanism for stagnation. Solute drag due to Fe impurities

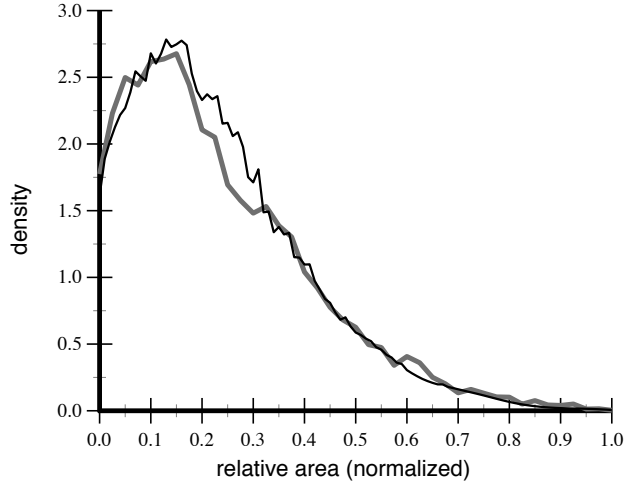

FIGURE 3. Relative area histograms from large scale simulation (thick gray) and from master equation (black)

cannot explain this behavior, but cf. [8]. Grooves are not expected to form in this film owing to the very stable oxide of *Al* which forms on exposure to air. In addition, grooving should pin boundaries with low curvature, but small grains, which by necessity have high curvature, are the most affected. Contributions other than grain boundary energy reduction can promote grain growth in thin films. Examples include surface, elastic strain, or plastic strain energies. Minimization of these energies typically promotes development of certain subpopulations of grains and leads to development of strong film texture. Here, however, the films initially had a strong $< 111 >$ texture and annealing resulted in minimally enhancing this texture. Finally, the films are in zero stress or low compressive steady state stress state at the annealing temperature. Thus film stress and relaxation are also not expected to play a significant role in observed grain growth and subsequent stagnation. To conclude, the orgins of film stagnation in the present context are not understood. Further, it is obvious that the film has not experienced what we generally interpret as normal grain growth.

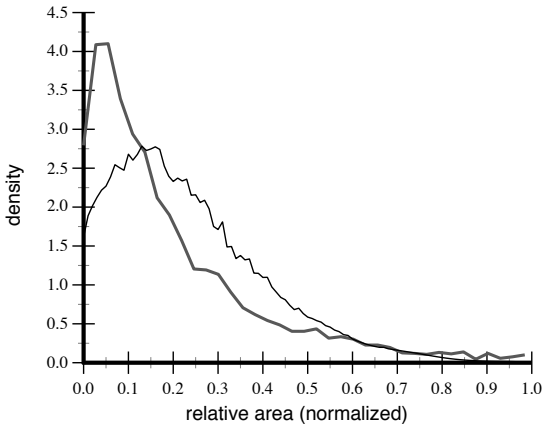

FIGURE 4. Comparison of normalized relative area probabilities for Al thin films (thick gray) at stagnation and the master equation simulation (black)

The simulation and the model of the simulation given by the master equation system we have discussed envisions a long time evolutionary process, so it is not surprising that their grain size statistics differ considerably from the experiment.

References

[1] Adams, B.L., Ta'asan, S., Kinderlehrer, D., Livshits, I., Mason, D., Wu, C., Mullins, W.W., Rohrer, G.S., Rollett, A.D., Saylor, D., 1999 *Extracting grain boundary energy from triple junction measurement*, Interface Science, 7, 321-338

[2] Barmak, K., Archibald, W., Kim, J., Kim, C.-S., Rollett, A.D., Rohrer, G. S., Ta'asan, S., and Kinderlehrer, D. *Grain boundary energy and grain growth in highly-textured Al films and foils: experiment and simulation*, Proc. ICOTOM

[3] Barmak, K., Archibald, W., Rollett, A.D., Ta'asan, S., and Kinderlehrer, D. *Grain boundary properties and grain growth: Al Foils, Al films*, MRS (to appear)

[4] Barmak, K., Kim, J., Archibald, W. E., Rohrer, G. R., Rollett, A. D., Kinderlehrer, D., Ta'asan, S., Zhang, H., and Srolovitz, D. *Grain boundary energy and grain growth in Al films: Comparison of experiments and simulations*

[5] Bronsard, L. and Reitich, F. 1993 *On three-phase boundary motion and the singular limit of a vector-valued Ginzburg-Landau equation*, Arch. Rat. Mech. Anal. 124, 355379

[6] Flyvbjerg, H. 1993 *Model for coarsening froths and foams*, Phys. Rev. E, 47, 4037-4054

[7] Fradkov, V.E. 1992 *Main Regularities of 2-D Normal Growth*, Material Science Forum, 94-96, pp. 269-274

[8] Gordon, P. and El-Bassayouni, T. E. 1965 *The effect of purity on grain growth in aluminum*, Trans. AIME, 233, 391-397

[9] Gurtin, M. 1993 *Thermomechanics of evolving phase boundaries in the plane*, Oxford

[10] Herring, C. 1951 *Surface tension as a motivatiion for sintering* in The Physics of Powder Metallurgy, (Kingston, W., ed.), McGraw Hill, 143 - 179

[11] Kinderlehrer, D. and Liu, C. 2001 *Evolution of Grain Boundaries*, Math. Models and Meth. Appl. Math. 11.4, pp. 713-729

[12] Kinderlehrer, D., Livshits, I., Manolache, F., Rollett, A. D., and Ta'asan, S. 2001 *An approach to the mesoscale simulation of grain growth*, Influences of interface and dislocation behavior on microstructure evolution, (Aindow, M. et al., eds), Mat. Res. Soc. Symp. Proc. 652, Y1.5

[13] Kinderlehrer, D., Lee, J., Livshits, I., Rollett, A.D., and Ta'asan, S. 2004 *Mesoscale simulation of grain growth, Recrystallization and Grain Growth*, Materials Science Forum vols 467-470, 1057-1062

[14] Kinderlehrer, D., Livshits, I., and Ta'asan, S. it A variational approach to modeling and simulation of grain growth to appear

[15] Kinderlehrer, D. and Tudorascu, A. *Mass transportation and transport*

[16] Mullins, W.W. 1956 *Two dimensional motion of idealized grain boundaries.* J. Appl. Phys., 27, 900 - 904

[17] Smith, C.S. 1948 *Grains, phases, and interfaces: an interpretation of microstructure*, Trans. Am. Inst. Mining Met. Eng. 175, 15 -51

[18] Thompson, C. V. 2001 *Grain growth and evolution of other cellular structures*, Solid State Physics, 55, 269-316

Katayun Barmak
Department of Materials Science and Engineering
Carnegie Mellon University
Pittsburgh, PA 15213 USA
e-mail: katayun@andrew.cmu.edu

David Kinderlehrer
David Kinderlehrer Department of Mathematical Sciences
Carnegie Mellon University
Pittsburgh, PA 15213 USA
e-mail: davidk@cmu.edu

Irine Livshits
Department of Mathematical Sciences
Ball State University
Muncie, IN 47306-0490 USA
e-mail: ilivshits@bsu.edu

Shlomo Ta'asan
Department of Materials Science and Engineering
Carnegie Mellon University
Pittsburgh, PA 15213 USA
e-mail: shlomo@andrew.cmu.edu